Egyptian Journal of Chemistry

http://ejchem.journals.ekb.eg/

Effects of both variable electrical conductivity and microstructural/multiple slips on MHD flow of micropolar nanofluid

M. E. Ouaf [a], M. Y. Abou-zeid [a*] and M. G. Ibrahim [b]

[a] *Department of Mathematics, Faculty of Education, Ain Shams University, Heliopolis, Cairo, 11757, Egypt.*

[b] *Department of Basic and Applied Science, Faculty of Engineering, IAEMS, 11311, Cairo, Egypt.*

Abstract

Through heating processes, electrical conductivity plays a crucial role in the food industry. The effects of Joule heating and temperature-dependent electrical conductivity on the boundary layer flow of micropolar fluid were the main topics of this paper. Considerations include thermal radiation, activation energy, and microstructural/multiple slips effects. The resulting partial differential equations system (PDEs) is transformed into a nonlinear ordinary differential equations model using the proper similarity variables (ODEs). The shooting technique, a highly reliable/accurate technique, is used to obtain semi-analytical results. In Mathematica13.1.1, apply the generalised differential transform method (GDTM), Dawar 2021 newly published results are used to approve/confirm the accuracy of the acquired results. Findings demonstrate that the parameter of temperature-dependent electrical conductivity enhances fluid temperature and increases energy gain in the heating operation system, which is important for the design of Ohmic heaters (food industry processes).

Keywords: Non-constant electrical conductivity; Microstructure/multiple slip; Activation energy; Micropolar fluid; Mathematica 13.1.1.

Introduction

When materials are cooled to extremely low temperatures, a phenomenon known as electrical conductivity/specific conductance takes place, where superconductors allow electricity to travel through without experiencing any electrical resistance. For the initial definition of electrical conductivity [1]. Kamerlingh Onnes conducted tests in 1911 to determine whether the Metal resistance at low temperatures would continue to drop linearly with the reduction in temperature or would be fixed at a particular value. The causes of electrical conductivity and its many applications, such as in electrical operations like particle accelerators, digital electrical circuits, and magnetic resonance imaging devices, as well as in medical processes like magnetic resonance, cables superconductivity, were first studied by researchers, investigators, and modelers [2–6]. Obalalu et al. [7] modification of the conductivity of electricity influence on the flow of Casson nanofluid was introduced in the context of fluids. They proposed that the link between fluid temperature and electrical conductivity is inverse. The impact of Joule dissipation in peristaltic nanofluid flow was instead researched by Qasim et al. [8]. They suggested that there is a direct correlation between electrical conductivity and fluid temperature. This work introduces a novel theoretical perspective on the relationship between fluid temperature and electrical conductivity. We should investigate the experimental relationship between electrical conductivity and fluid temperature before making a judgement regarding this relationship. As a result, every experiment that has been done has demonstrated a connection between electrical conductivity and fluid temperature.

In applications like micro-pumps, hard disc drives, micro-valves, and nozzles, slip flows are regarded as the most important problem of microsystems. Dawar et al. [9] investigate the impact of first and second-order slip flow on the MHD micropolar boundary layer flow. They claimed that compared to a non-microstructural slip, a microstructural slip has a greater visible effect on the distribution of velocity due to high magnetic parameter values. Mabood and Shateyi [10] thought carefully about the effects of heat radiation and numerous slips on an unstable flow with sheets that are stretched. They discovered that the slip parameter's values result in a drop in fluid velocity close to the

* Corresponding author should be addressed: mohamed_abouzid@edu.asu.edu.eg

Receive Date: 30 December 2022, **Revise Date:** 16 January 2023, **Accept Date:** 17 January 2023

First Publish Date: 18 January 2023

DOI: 10.21608/EJCHEM.2023.184388.7407

boundary layer. Mahmoud and Waheed [11] discussed how magnetic fields affect micropolar fluid flow. Afzal and Aziz [12] investigated the impact of MHD slip and changing thermal conductivity on nanofluid flow with heat and mass transfer. Numerous researchers and modelers have explored the effects of slip on flow and its applications in this direction [13-20].

We selected a highly numerical methodology termed by shooting method combination with Runge-Kutta method to produce the results/solutions of the MHD boundary layer flow of micropolar fluid that are provided in the current work (ODE45). The shooting method is typically thought of as a highly constructive method in numerical analysis that uses dropping the boundary value problem to an initial value problem to solve it. Up until a solution is found that also fulfils the boundary value problem's boundary conditions, it entails finding initial value problem solutions for a variety of initial conditions. Merle proposed the shooting method in 1988 [21], and it was he who found the solution to the nonlinear Dirac equations. The shooting technique was first used by Hasanuzzaman et al. [22] to solve the Problem with MHD boundary layer flow involving the influence of transpiration. MHD Casson Nanofluid Laminar Boundary Layer Flow was investigated by Lanjwani et al [23] using the shot method. The shooting approach is frequently used by authors and researchers to find answers to numerous boundary value problems [24–28].

The primary goal of this investigation is to provide a novel theoretical framework for the impacts of temperature-dependent electrical conductivity, microstructure, and multiple slips on the MHD boundary layer flow of micropolar fluid by employing a very precise method known as the shot method. The proposed model's solution is presented in two separate scenarios, the first involving a viscous fluid (α=0), and the second using a micropolar fluid (α=1). Results for temperature gradients, velocity gradients, and distributions of the concentration of nanoparticles are provided in various mentioned instances. With the help of Mathematica 13.1.1 and advanced shooting method algorithms, the findings given were obtained.

Experimental

Consideration is given to the flow of micropolar fluid within a stretching sheet. Conditions for a microstructure slide are taken into account. The velocity of the stretching sheet is supposed to $us = ax$ where (a) the stretching rate. Applied magnetic field B_0 strength in the y-axis of constant value. In view of the formulated problem, the governing equations can take the form [20]:

$$\frac{\partial u'}{\partial x'} + \frac{\partial v'}{\partial y'} = 0, \quad (1)$$

$$u'\frac{\partial u'}{\partial x'} + v'\frac{\partial u'}{\partial y'} = \frac{\kappa}{\rho}\frac{\partial N'}{\partial y'} + \frac{\partial^2 u'}{\partial y^{2'}} - \frac{\sigma(T',C')B_0^2}{\rho}u' + g\{\beta_C(C' - C'_\infty) + \beta_T(T' - T'_\infty)\}, \quad (2)$$

$$u'\frac{\partial N'}{\partial x'} + v'\frac{\partial N'}{\partial y'} = \frac{\Omega}{\rho_j}\frac{\partial^2 N'}{\partial y^{2'}} - \frac{\kappa}{\rho_j}\left(2N' + \frac{\partial N'}{\partial y'}\right), \quad (3)$$

$$u'\frac{\partial T'}{\partial x'} + v'\frac{\partial T'}{\partial y'} = \frac{k}{\rho c_p}\left(1 + \frac{16}{3}\frac{\sigma^* T_0^3}{kk^*}\right)\frac{\partial^2 T'}{\partial y^{2'}} + \frac{\sigma(T',C')B_0^2}{\rho c_p}u^{2'} + \tau\left[D_B\frac{\partial T'}{\partial y'}\frac{\partial C'}{\partial y'} + \frac{D_B}{D_T}\left(\frac{\partial T'}{\partial y'}\right)^2\right], \quad (4)$$

$$u'\frac{\partial C'}{\partial x'} + v'\frac{\partial C'}{\partial y'} = D_B\frac{\partial^2 C'}{\partial y^{2'}} + K_r^2(C' - C'_\infty)\left(\frac{T'}{T'_\infty}\right)^n e^{\left(\frac{-E'_a}{K_B T'}\right)}. \quad (5)$$

Where, the spin (Ω) gradient velocity which defined as the follows:

$$\Omega = \mu\left(1 + \frac{\alpha}{2}\right)j, \quad (6)$$

Here, the micropolar ($\alpha = \frac{\kappa}{\mu}$) parameter.

The chosen/appropriate boundary conditions are described as follows [9]:

$$u' = u_s + u_{slip}, v' = 0, N' - n\frac{\partial u'}{\partial y'}, T' = T'_s, C' = C'_s \text{ at } y = 0, \quad (7)$$

$$u' \to 0, N' \to 0,\ T' \to T'_\infty, \text{ and } C' \to C'_\infty \text{ as } y \to \infty \quad (8)$$

Here, the micro-rotation (n) parameter, the fluid (C, C_s) nanoparticles concentration and nanoparticles concentration near the surface, the ambient fluid (C_∞) nanoparticles concentration, the coefficient of (D_B) Brownian diffusion, the coefficient of thermophoretic (D_T) diffusion, the gravitational (g) acceleration, the thermal (k) conductivity, the coefficient of mean (k^*) absorption, the Stefan-Boltzmann (σ^*) constant, the fluid (T, T_s) temperature and temperature near to the surface, the nanoparticles concentration (β_C) expansion, the thermal (β_T) expansion, the vortex (κ) viscosity, the dynamic (μ) viscosity. $\sigma(T', C')$ is the variable electrical conductivity, which defined as:

$$\sigma = \sigma_0\left[1 + \epsilon\left(\frac{T' - T'_\infty}{T'_s - T'_\infty}\right) + \beta\left(\frac{C' - C'_\infty}{C' - C'_\infty}\right)\right], \quad (9)$$

Here, σ_0 is the constant electrical conductivity case, ϵ is the temperature-dependent electrical conductivity parameter and β is the nanoparticles concentration-dependent electrical conductivity parameter.

The appropriate transformations are proposed:

$$\psi = \sqrt{avx}f'(\eta), u = \frac{\partial\psi}{\partial y}, v = \frac{\partial\psi}{\partial x}, N = ax\sqrt{\frac{a}{2v}}g(\eta),$$

$$\eta = y\sqrt{\frac{a}{v}}y, \theta(\eta) = \frac{T' - T'_\infty}{T'_s - T'_\infty} \text{ and } \phi(\eta) = \frac{C' - C'_\infty}{C' - C'_\infty}. \quad (10)$$

Here η is the similarity variable, $f(\eta)$ is the non-dimensional stream function, $f'(\eta)$ axial velocity, $\theta(\eta)$ is the temperature, $g(\eta)$ is the micropolar particles rotation, and $\phi(\eta)$ nanoparticles volume fraction, correspondingly. The governing system of differential equations are transformed/ non-dimensional as follows.

$$(1 + \alpha)f''' + ff'' - f'^2 - \alpha g' + \gamma_1\theta + \gamma_2\varphi - M(1 + \epsilon\theta + \beta\varphi)f' = 0, \quad (11)$$

$$\left(1 + \frac{\alpha}{2}\right)g'' + fg' - gf' - \alpha(f'' + 2g) = 0, \quad (12)$$

$\frac{(1+R_d)\theta''}{P_r} + Nb\,\theta'\phi' + Nt\,\theta'^2 + S\,\theta + E_c\,(1+\alpha)f'''^2 + f\theta' + M\,(1+\epsilon\,\theta+\beta\varphi)\,E_c\,f'^2 = 0,$ (13)

$\varphi'' + f\varphi'(\eta) + \frac{N_t}{N_b}\theta''(\eta) - P_r L_e\big(1+\delta\,\theta(\eta)\big)^n e^{\left(\frac{-E}{1+\delta\,\theta(\eta)}\right)}\varphi(\eta) = 0.$ (14)

With boundary conditions:

$f(0)=0, f'(0)=1+\gamma f''(0)+\delta_1 f'''(0)+R_0\,g'(0),\ g(0)=-mf'', \theta(0)=1, \phi(0)=1,$ (15)

$f'(\infty)=0, g(\infty)=0,\ \theta(\infty)=0, \phi(\infty)=0.$ (16)

Where, $M=\frac{2\sigma_0 B_0^2}{\rho\,a}$ is the Hartmann number, $K_p=\frac{2\,\upsilon}{a\,K\,p_0}$ is the porous parameter $P_r=\frac{\upsilon}{\alpha}$ is the Prandtl number,$R_d=\frac{16\,\sigma^*\,T_\infty^3}{3\,k\,k^*}$ is the radiation parameter $E_c=\frac{u_s^2}{c_p\,(T_s-\,T_\infty)}$ is the Eckert number, $S=\frac{2\iota Q_0}{a\rho C_p}$,is the heat source factor $Nb=\frac{\tau D_B\,(C_w-\,C_\infty)}{\upsilon}$ is the Brownian motion parameter, $Nt=\frac{\tau D_T\,(T_s-\,T_\infty)}{\upsilon T_\infty}$ is the thermophoresis parameter, $\lambda=\frac{v_0}{\sqrt{av}}$ is the transpiration parameter, species, $L_e=\frac{\nu}{D_B}$ is the Lewis number, $\delta=\frac{T_s'-T_\infty'}{T_\infty'}$ is the temperature difference parameter and $E=\frac{E_a}{K_B T'}$ is the Activation energy.

By using the proper similarity variables and boundary conditions, the ordinary differential equations system (11–14) is transformed into a nondimensional system (15-16). Utilizing the superposition technique, the Higher-order values are extracted using the GDTM technique after obtaining the initial conditions and first order of the differential equation. The answers of differential equations system can be obtained accurately and efficiently using this method [29–31].

The general n[th] order ordinary differential equation can be written as:

$y(t,f,f',\ldots,f^{(n)})=0.$ (17)

This equation is subjected to the initial guess.

$f^{(k)}(0)=d_k,\ k=0,\ldots,n-1.$ (18)

Let $f(t)$ be analytic in a domain D and let $t=t_0$ represent any point in D. The k^{th} derivative transformation of a function $f(t)$ can be defined as follows:

$F(k)=\left(\frac{1}{k!}\right)\left[\left(\frac{d^{(k)}f(t)}{dt^{(k)}}\right)\right]_{(t=t^0)},\ \forall t\in D.$ (19)

Results and discussion

Here, the velocity, micro-rotation velocity, temperature, and nanoparticle concentration are numerically analysed for different values of the physical components involved in the problem to emphasise the implications of these parameters in more detail. The values listed below are also used as the benchmark for these parameters:

$\alpha=0.1, Nb=0.2,\ Nt=0.3, S=0.2, \gamma_1=1, \gamma_2=0.8, E_c=0.2\ \epsilon=0.2, \beta=0.2, E=2, \delta=0.1, R_d=1, \gamma=0.7, m=0.4, \delta_1=-1, R_0=0.1, P_r=1, L_e=0.2$

The dimensionless viscosity ratio α measures the relative strengths of the vortex viscosity coefficient to the viscosity coefficient. The coefficients listed here are higher than or equal to 0. For example, the blood, $\alpha=0.08$. Figs. (1) and (2) show the change of the velocity f' versus the dimensionless coordinate η for different values of thermal Grashof number γ_1 and the dimensionless viscosity ratio α in case of temperature and nanoparticles concentration depend on electrical conductivity, respectively. It is seen, from these figures that the velocity increases with the increase of γ_1, whereas it decreases as α increases, this is due to the fact that the effect of the viscosity coefficient on fluid flow creates a resistance force which may decreases the fluid motion. For large values of α, the velocity decreases with η till a definite value $\eta=\eta_0$ (represents the minimum value of f') and it increases afterwards. The effects of the slip velocity parameter γ on the velocity which is a function of η are shown in Fig. (3). It is found that the velocity f' distribution decreases by increasing γ in the interval $\eta\in[0, 2.4]$; otherwise, it increases by increasing η. So, the behavior of g in the interval $\eta\in[0, 2.4]$, is an inversed manner of its behavior in the interval $\eta\in[2.4, 5]$ except that the curves are very close to each other than those obtained in the first interval.

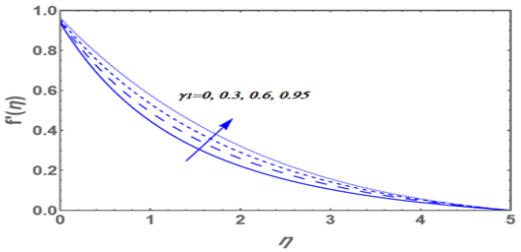

Fig.1 The velocity component is plotted against η for the variation value of γ_1.

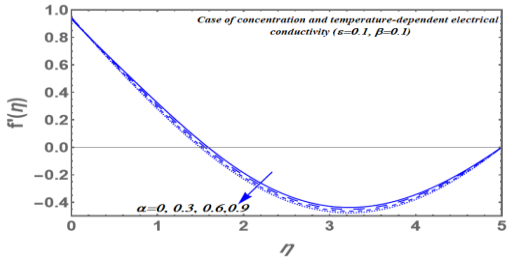

Fig. 2 The velocity component is plotted against η for the variation value of α.

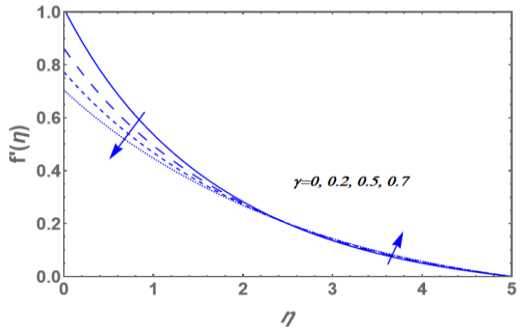

Fig.3. the velocity component is plotted against η for the variation value of γ.

The effects of the dimensionless viscosity ratio α in case of temperature and nanoparticles concentration don't depend on electrical conductivity on the microrotation g which is a function of η are shown in Fig. (4). It is found that the microrotation distribution increases by increasing α. Moreover, for large values of α, the microrotation increases with η till a definite value $\eta = \eta_0$ (represents the maximum value of g) and it decreases afterwards. Figs. (5) and (6) show the behavior of the microrotation g with the dimensionless coordinate η for various values of the magnetic field parameter M and the thermophoresis parameter Nt, respectively. It has been noticed that the microrotation distribution increases by increasing M in the interval $\eta \in [0, 1.3]$; otherwise, it decreases by increasing η. While the effect of Nt is to decrease g in the interval $\eta \in [0, 2.1]$, and it has an inversed manner in the interval $\eta \in [2.1, 5]$ except that the curves are very close to each other than those obtained in the first interval. In this case, for large values of M, and small values of Nt there is a maximum value of g holds at $\eta \cong 0.4$. The effects of the other parameters are recorded to be similar to them; these figures are left out here to avoid repetition.

Figs. (7) and (8) show the behavior of the temperature θ with the dimensionless coordinate η for various values of the thermophoresis parameter Nt and thermal Grashof number γ_1, respectively. It has been noticed that the temperature increases with the increases of Nt, while it decreases as γ_1 increases. It is also noted that for each value of both Nt and γ_1, θ decrease as η increases and the relation between θ and η seems as a hyperbolic.

The result in Fig. (7) is caused by the thermophoresis effect, which is a force caused by the temperature difference between the hot liquid and the cold wall that moves the particles towards the cold wall.

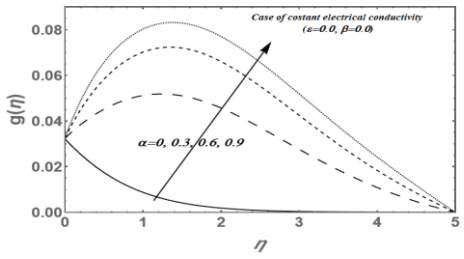

Fig. 4 The microrotation velocity is plotted against η for the variation value of α.

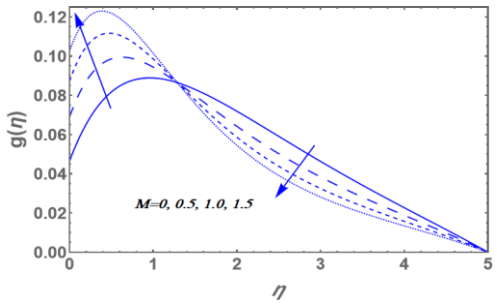

Fig. 5 The microrotation velocity is plotted against η for the variation value of M.

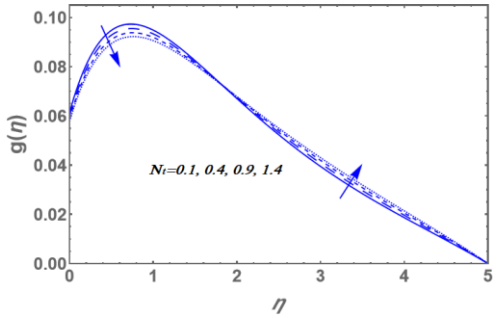

Fig. 6 The microrotation velocity is plotted against η for the variation value of Nt.

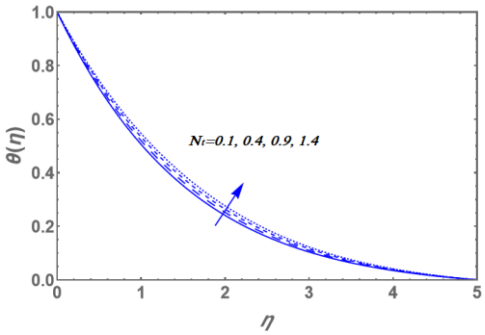

Fig. 7 The temperature is plotted against η for the variation value of Nt.

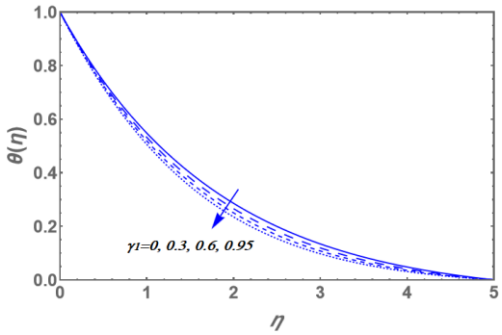

Fig. 8 The temperature is plotted against η for the variation value of γ_1.

The variations of the nanoparticle's concentration distribution φ with the dimensionless coordinate η for various values of activation energy parameter Ea and the reaction parameter σ are displayed in Figs. (9) and (10), respectively. The graphs in Figs. (9) and (10) show that as the parameter Ea is increased, the nanoparticle concentration distribution also increases. while it decreases by increasing the parameter α, respectively. It is also noted that for small values of Ec and large values of σ, the relation between φ and η is a parabola, i.e. φ increases with η till a definite value $\eta = \eta_0$ (represents the maximum value of φ) and it decreases afterwards. This maximum value of φ increases by increasing Ea, while it decreases by increasing σ. The results which are obtained in Fig. (10), are consistent with the findings of Eldabe et al. [32]. Other parameters have an effect on the temperature, but they are recorded to be similar to those obtained in Fig. (9) and (10). In order to preserve space, figures are not included here. Figure (11) displays the effect of magnetic field parameter M on the nanoparticle's concentration distribution φ which is a function of η. It is found that the nanoparticles concentration decreases by increasing M in the interval $\eta \in$ [0, 1.43]; otherwise, it increases by increasing η. So, the behavior of φ in the interval $\eta \in$ [0, 1.43], is an inversed manner of its behavior in the interval $\eta \in$ [1.43, 5], and in the first interval, there is a maximum value of φholds at η =0.44.

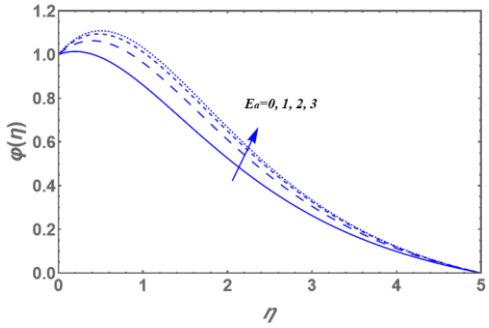

Fig. 9 The nanoparticles concentration is plotted against η for the variation value of Ea.

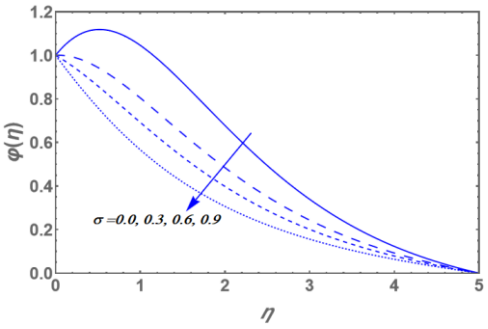

Fig. 10 The nanoparticles concentration is plotted against η for the variation value of σ.

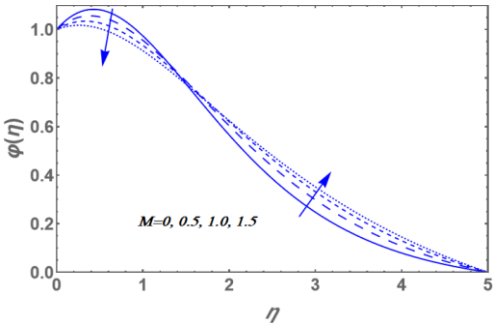

Fig. 11 The nanoparticles concentration is plotted against η for the variation value of M.

Conclusion

The activation energy effect as well as temperature and nanoparticle concentration-dependent conductivity are both included in this problem, expanding upon the work of [20]. The velocity, temperature, and concentration extremely nonlinear partial differential equations are transformed into nonlinear ordinary differential equations using the appropriate transforms. By using DTM and a program from the MATHEMATICA package, we were able to numerically solve this set of equations. The current analysis can act as a model that could aid in understanding physiological flux mechanics [33–53]. Following is a summary of the results that were attained.

1. By increasing both Nt and γ_1, the velocity increases while it decreases as α, M and β increase. Moreover, it increases or decreases as γ increases.
2. The microrotation velocity distribution increases or decreases as Nt, γ_1, α, M, γ and β increase.
3. The microrotation velocity becomes greater with increasing the dimensionless coordinate η and reaches maximum value, after which, it decreases.
4. The temperature distribution increases as Nt, α, M, γ and β increase, while it decreases when γ_1 increases. Furthermore, it increases or decreases as the problem's other physical parameters increase.
5. The nanoparticles concentration behavior is contrary with respect to the temperature behavior except that it decreases as α and σ increase.

Acknowledgment

The authors would like to express their sincere gratitude to the anonymous referee for her useful comments.

Conflict of interest

The authors have declared that this paper has no conflict of interest.

References

[1] T. Sakai, G. Adachi and J. Shiokawa, Electrical conductivity of Ln VO 3 compounds, 11, (1976) 1295-1300.

[2] N. T. M. Eldabe, M. Y. Abou-zeid, M. E. Ouaf, D. R. Mustafa and Y. M. Mohammed, Cattaneo – Christov heat flux effect on MHD peristaltic transport of Bingham nanofluid through a non – Darcy porous medium Int. J. Appl. Electromag. Mech. 68 (2022), 59-84.

[3] Abuiyada, A. J., Eldabe, N. T., Abouzeid, M. Y., Elshabouri, S., Effects of thermal diffusion and diffusion thermo on a chemically reacting MHD peristaltic transport of Bingham plastic nanofluid. Journal of Advanced Research in Fluid Mechanics and Thermal Sciences 98 (2) (2022), 24-43.

[4] Mohamed, Y.M., El-Dabe, N.T., Abou-zeid, M.Y., Oauf, M.E., Mostapha, D.R., Effects of thermal diffusion and diffusion thermo on a chemically reacting MHD peristaltic transport of Bingham plastic nanofluid. Journal of Advanced Research in Fluid Mechanics and Thermal Sciences 98 (1) (2022), 1-17.

[5] Shaaban, A. A. & Abou-zeid, M. Y. Effects of heat and mass transfer on MHD peristaltic flow of a non-Newtonian fluid through a porous medium between two coaxial cylinders. Math. Probl. Eng. **2013**, 819683 (2013).

[6] Eldabe N.T., Abo-zeid M. Y., Younis Y. M. Magnetohydrodynamic peristaltic flow of Jeffry nanofluid with heat transfer through a porous medium in a vertical tube. *Appl. Math. Inf. Sci*. **11**, 1097-103 (2017).

[7] A. M. Obalalu, O. A. Ajala, A. Abdulraheem, and A. O. Akindele, The influence of variable electrical conductivity on non-Darcian Casson nanofluid flow with first and second-order slip conditions, Partial Differential Equations in Applied Mathematics 4 (2021) 100084.

[8] M. Qasim, Z. Ali, A. Wakif and Z. Boulahia, Numerical Simulation of MHD Peristaltic Flow with Variable Electrical Conductivity and Joule Dissipation Using Generalized Differential Quadrature Method, Commun. Theor. Phys. 71 (2019) 509–518.

[9] A. Dawar, Z. Shah, A. Tassaddiq, S. Islam, and P. Kumam, Joule heating in magnetohydrodynamic micropolar boundary layer flow past a stretching sheet with chemical reaction and microstructural slip, Case Studies in Thermal Engineering 25 (2021) 100870.

[10] F. Mabood and S. Shateyi, Multiple Slip Effects on MHD Unsteady Flow Heat and Mass Transfer Impinging on Permeable Stretching Sheet with Radiation, Modelling and Simulation in Engineering, Volume 2019, Article ID 3052790, 1-11.

[11] M. Mahmoud and S. Waheed, Effects of slip and heat generation/absorption on MHD mixed convection flow of micropolar fluid over a heated stretching surface, Math. Probl Eng., vol. 2010, pp. 1–20, ID 579162, 2010.

[12] K. Afzal and A. Aziz, Transport, and heat transfer of time dependent MHD slip flow of nanofluids in solar collectors with variable thermal conductivity and thermal radiation, Results in Physics, 6 (2016) 1-8.

[13] E. Hosseini, G. B. Loghmani, M. Heydari, M.M. Rashidi, Numerical investigation of velocity slip and temperature jump effects on unsteady flow over a stretching permeable surface, De European Physical Journal Plus 132 (2) (2017) 96.

[14] N. T. Eldabe, M. Y. Abou-zeid, M. A. Mohamed and M. Maged, Peristaltic flow of Herschel Bulkley nanofluid through a non-Darcy porous medium with heat transfer under slip condition, International Journal of Applied Electromagnetics and Mechanics 66 (2021), 649-668.

[15] M. E. Ouaf, M. Y. Abouzeid and Y. M. Younis, Entropy generation and chemical reaction effects on MHD non-Newtonian nanofluid flow in a sinusoidal channel, International Journal of Applied Electromagnetics and Mechanics, 69 (2022), 45-65.

[16] M. Y. Abouzeid, Chemical reaction and non-Darcian effects on MHD generalized Newtonian nanofluid motion, Egyptian Journal of Chemistry, 65(12) (2022), 647-655.

[17] M. Sohail, U. Ali, Q. Al-Mdallal, et al., Theoretical and numerical investigation of entropy for the variable thermophysical characteristics of couple stress material: applications to optimization, Alexandria Engineering Journal 59 (6) (2020) 4365–4375.

[18] M. Y. Abou-zeid, and M. A. A. Mohamed, Homotopy perturbation method for creeping flow of non-Newtonian Power-Law nanofluid in a nonuniform inclined channel with peristalsis. Z. Naturforsch 72 ((10)a) (2017), 899–907.

[19] R. Ellahi, Exact solutions of flows of an oldroyd 8-constant fluid with nonlinear slip conditions, Zeitschrift für Naturforschung A, 65 (12) (2010) 1081–1086.

[20] N. T. M. Eldabe, M. Y. Abouzeid, and H.A. Ali, Effect of heat and mass transfer on Casson fluid flow between two co-axial tubes with peristalsis, J. Adv. Res. Fluid Mech. Therm. Sci. 76(1) 2020 54-75.

[21] F. Merle, Existence of stationary states for nonlinear Dirac equations, Journal of Differential Equations, 74 (1988), 50–68.

[22] M. D. Hasanuzzaman, M. D. A. Kabir and M. D. T. Ahmed, Transpiration effect on unsteady natural convection boundary layer flow around a vertical slender body, Results in Engineering, 12 (2021)100293.

[23] H. B. Lanjwani, M. S. Chandio, M. I. Anwar, S. A. Shehzad and M. Izadi, MHD Laminar Boundary Layer Flow of Radiative Fe-Casson Nanofluid: Stability Analysis of Dual Solutions, Chinese Journal of Physics, (2021), In Press.

[24] M. E. Ouaf and M. Abou-zeid, Electromagnetic and non-Darcian effects on a micropolar non-Newtonian fluid boundary-layer flow with heat and mass transfer, International Journal of Applied Electromagnetics and Mechanics 66 (2021), 693-703.

[25] N. T. Eldabe, M. Y. Abou-zeid, O. H. El-Kalaawy, S. M. Moawad and O.S Ahmed, Electromagnetic steady motion of Casson fluid with heat and mass transfer through porous medium past a shrinking surface, Thermal Science 25(1A) (2021), 257-265.

[26] N. T. M. Eldabe, M. Y. Abou-zeid, S. M. Elshabouri, T. N. Salama and A. M. Ismael, Ohmic and viscous dissipation effects on micropolar non-Newtonian nanofluid Al2O3 flow through a non-Darcy porous media, International Journal of Applied Electromagnetics and Mechanics 68 (2022), 209-221.

[27] N. T. M. Eldabe, R. R. Rizkallah, M. Y. Abouzeid and V. M. Ayad, Thermal diffusion and diffusion thermo effects of Eyring- Powell nanofluid flow with gyrotactic microorganisms through the boundary layer, Heat Transfer - Asian Res. 49 (2020), 383 – 405.

[28] N. T. Eldabe, G. M. Moatimid, M. Y. Abouzeid, A. A. ElShekhipy and N. F. Abdallah, A semianalytical technique for MHD peristalsis of pseudoplastic nanofluid with temperature-dependent viscosity: Application in drug delivery system, Heat Transfer-Asian Research 49 (2020), 424– 440.

[29] N. T. M. Eldabe, G. M. Moatimid, M. Abou-zeid, A. A. Elshekhipy and N. F. Abdallah, Semi-analytical treatment of Hall current effect on peristaltic flow of Jeffery nanofluid, International Journal of Applied Electromagnetics and Mechanics 7 (2021), 47-66.

[30] N. T. M. Eldabe, G. M. Moatimid, M. Abou-zeid, A. A. Elshekhipy and N. F. Abdallah, Instantaneous thermal-diffusion and diffusion-thermo effects on Carreau nanofluid flow over a stretching porous sheet, Journal of Advanced Research in Fluid Mechanics and Thermal Sciences, Volume 72, Issue 2, 2020, Pages 142-157.

[31] M. Ibrahim, N. Abdallah and M. Abouzeid, Activation energy and chemical reaction effects on MHD Bingham nanofluid flow through a non-Darcy porous media, Egyptian Journal of Chemistry Doi: 10.21608/EJCHEM.2022.117814.5310.

[32] N. T. M. Eldabe, M. Y. Abou-zeid, A. Abosaliem, A. Alana, and N. Hegazy, Thermal Diffusion and Diffusion Thermo Effects on Magnetohydrodynamics Transport of Non-Newtonian Nanofluid Through a Porous Media Between Two Wavy Co-Axial Tubes, **IEEE** Transactions on Plasma Science, 50 (2021), 1282-1290.

[33] N. T. M. Eldabe, M. Y. Abou-zeid, A. Abosaliem, A. Alana, and N. Hegazy, Homotopy perturbation approach for Ohmic dissipation and mixed convection effects on non-Newtonian nanofluid flow between two co-axial tubes with peristalsis, International Journal of Applied Electromagnetics and Mechanics 67 (2021), 153-163.

[34] M. Y. Abou-zeid, Homotopy perturbation method to gliding motion of bacteria on a layer of power-law nanoslime with heat transfer, Journal of Computational and Theoretical Nanoscienc, 12 (2015), 3605–3614.

[35] N. T. M. Eldabe, M. Y. Abou-zeid, Radially varying magnetic field effect on peristaltic motion with heat and mass transfer of a non-Newtonian fluid between two co-axial tubes Thermal science, 22 (2018) 2449-2458

[36] M. Y. Abou-zeid, Homotopy perturbation method for couple stresses effect on MHD peristaltic flow of a non-Newtonian nanofluid, Microsystem Technologies, 24 (2018) 4839–4846

[37] Nabil T. M. Eldabe, Mohamed A. Hassan and Mohamed Y. Abou-zeid, Wall properties effect on the peristaltic motion of a coupled stress fluid with heat and mass transfer through a porous medi, Journal of Engineering Mechanics, 142 (2015) 04015102.

[38] T. Eldabe, S. Elshabouri, H. Elarabawy, M. Y. Abouzeid and A. J. Abuiyada, Wall properties and Joule heating effects on MHD peristaltic transport of Bingham non-Newtonian nanofluid, International Journal of Applied Electromagnetics and Mechanics, 69 (2022), 87 – 106.

[39] M. E. M. Ouaf and M. Y. Abou-zeid, Hall currents effect on squeezing flow of non-Newtonian nanofluid through a porous medium between two parallel plates, Case Studies in Thermal Engineering, 28 (2021), 101362.
[40] N. T. M. Eldabe, M. Y. Abou-zeid, M. A. A. Mohamed and M. M. Abd-Elmoneim, MHD peristaltic flow of non-Newtonian power-law nanofluid through a non-Darcy porous medium inside a non-uniform inclined channel, Archive of Applied Mechanics, 91 (2021), 1067–1077.
[41] M. Y. Abou-zeid, Implicit homotopy perturbation method for MHD non-Newtonian nanofluid flow with Cattaneo-Christov heat flux due to parallel rotating disks, Journal of nanofluids, 8 (8) (2019), 1648-1653.
[42] N. T. Eldabe, A. A. Shaaban, M. Y. Abou-Zeid, H. A. Ali, Magnetohydrodynamic non-Newtonian nanofluid flow over a stretching sheet through a non-Darcy porous medium with radiation and chemical reaction, Journal of Computational and Theoretical Nanoscience, 12 (2015), 5363-٥٣71.
[43] M. A. Mohamed and M.Y. Abou-zeid, MHD peristaltic flow of micropolar Casson nanofluid through a porous medium between two co-axial tubes, Journal of porous media, 22 (2019), 1079–1093.
[44] N. T. M. Eldabe, R. R. Rizkallah, M. Y. Abou-zeid and V. M. Ayad, Effect of induced magnetic field on non-Newtonian nanofluid Al_2O_3 motion through boundary-layer with gyrotactic microorganisms, Thermal Science, 26 (2022), 411 – 422.
[45] N.T. Eldabe, M.Y. Abou-zeid and H. A. Shawky, MHD peristaltic transport of Bingham blood fluid with heat and mass transfer through a non-uniform channel, J. Adv. Res. Fluid Mech. Thermal Science, 77 (2021), 145–159.
[46] A. Ismael, N. Eldabe, M. Abouzeid and S. Elshabouri, Activation energy and chemical reaction effects on MHD Bingham nanofluid flow through a non-Darcy porous media, Egyptian Journal of Chemistry, 65 (2022), 715 – 722.
[47] N. T. El-Dabe, M.Y. Abouzeid and O.S. Ahmed, Motion of a thin film of a fourth grade nanofluid with heat transfer down a vertical cylinder: Homotopy perturbation method application, Journal of Advanced Research in Fluid Mechanics and Thermal Sciences 66 (2) (2020), 101-113.
[48] Ismael, A.M., Eldabe, N.T.M., Abou-zeid, M.Y. & Elshabouri, S.M. Thermal micropolar and couple stresses effects on peristaltic flow of biviscosity nanofluid through a porous medium. Sci. Rep. 12,16180 (2022).
[49] Ibrahim, M. G. and Abou-zeid, M.Y. Influence of variable velocity slip condition and activation energy on MHD peristaltic flow of Prandtl nanofluid through a non-uniform channel. Sci. Rep. 12,18747 (2022).
[50] Mansour, H.M., Abou-zeid, M.Y., Heat and mass transfer effect on non-Newtonian fluid flow in a non-uniform vertical tube with peristalsis. J. Adv. Res. Fluid Mech. Therm. Sci. 61(1), 44–62 (2019).
[51] Abou-zeid, M.Y. Homotopy perturbation method for MHD non-Newtonian nanofluid flow through a porous medium in eccentric annuli in peristalsis. Thermal Sci. **5**, 2069-2080 (2017).
[52] Abou-zeid, M.Y., Shaaban, A.A. and Alnour, M.Y. Numerical treatment and global error estimation of natural convective effects on gliding motion of bacteria on a power-law nanoslime through a non-Darcy porous medium, Journal of Porous Media 18 (2015), 1091–1106.
[53] M.Y. Abou-zeid, Magnetohydrodynamic boundary layer heat transfer to a stretching sheet including viscous dissipation and internal heat generation in a porous medium, J. Porous Media 14 (2011), 1007-1018.